ACS OMEGA

http://pubs.acs.org/journal/acsodf

Article

Predicting Pyrolysis of a Wide Variety of Petroleum Coke Using an Independent Parallel Reaction Model and a Backpropagation Neural Network

Jindi Huang, Zhihang Chen, Dou Zhang, and Jing Li*

Cite This: *ACS Omega* 2022, 7, 41201−41211

Read Online

ACCESS | Metrics & More | Article Recommendations | Supporting Information

ABSTRACT: In this work, the pyrolysis behavior and gaseous products of petroleum coke were investigated by nonisothermal thermogravimetric analysis (TGA) and thermogravimetry−mass spectrometry (TG−MS). Then, the pyrolysis kinetics of six kinds of petroleum coke (Fushun (FS), Fuyu (FY), Wuhan (WH), Zhenhai (ZH), Qilu (QL), and Shijiazhuang (SJZ)) were determined by an independent parallel reaction (IPR) model, and the kinetic parameters (activation energy and preexponential factor) were obtained. In addition, an efficient backpropagation neural network (BPNN) was developed to predict the thermal data of six kinds of petroleum coke. The BPNN-predicted thermal data were used to calculate the kinetic parameters based on the IPR model, and the results were compared with the ones calculated using experimental data. The results showed that the pyrolysis process of six kinds of petroleum coke was divided into three stages, of which stage II (250−900 °C) had the significant mass loss, corresponding to the devolatilization of petroleum coke. MS fragmented ion intensity analysis indicated that the main pyrolysis products were methane CH_x (m/z = 13, 14, 15, and 16), aliphatic hydrocarbon C_3H_5, H_2, CO, CO_2, and H_2O. The thermal data predicted by the IPR, BPNN, and BPNN-IPR (BPNN combined with IPR) models were in good agreement with the experimental data. Most importantly, it was concluded that the BPNN-predicted data can be further applied to calculate the kinetic parameters using the IPR kinetic model.

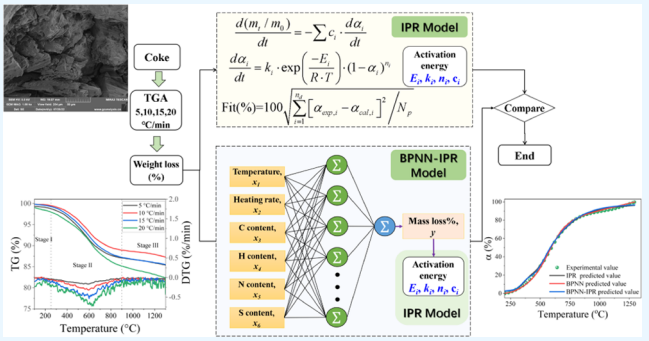

1. INTRODUCTION

Petroleum coke is a byproduct of the oil refining process and has a high carbon content and calorific value. It is widely used as an important industrial raw material to produce carbon products such as prebaked anodes, graphite electrodes, and carburizing agents after high-temperature calcination, as well as fuel after gasification.[1−9] In recent years, with the progress of heavier, degraded, and deep processing of crude oil around the world, the output of petroleum coke has increased significantly. It is reported that the global output of petroleum coke has exceeded 150 million tons, and China is one of the major petroleum coke consumers.[10−13] Worldwide, rotary kilns and vertical shaft calciners are the main calcination equipment of petroleum coke, and more than 70% of petroleum coke in China is calcined by a vertical shaft calciner. In the calcining process of petroleum coke by a vertical shaft calciner, a large amount of volatile matter is released, and the precipitated volatiles enter the calciner combustion system to participate in the combustion. Volatile combustion heat accounts for 50% of the entire calcination energy consumption and is an important heat source in the calcination process. Relevant studies have shown that factors such as calcination temperature, heating rate, particle size, and sample characteristics directly affect the migration and transformation paths of petroleum coke pyrolysis volatiles (light gas, tar, etc.), which in turn affect the quality of calcined coke.[14−16] Therefore, it is of great significance to precisely grasp the pyrolysis kinetics of petroleum coke to control the fuel supply in the calcination process, improve product quality, and reduce energy consumption.

To date, some related studies on the pyrolysis kinetics of petroleum coke have been reported. Shen et al.[17] proposed introducing a $(1-\alpha)^3$ model to predict the pyrolysis process of petroleum coke and estimated the kinetic parameters of four kinds of petroleum coke. Afrooz et al.[18] proposed using five different models to estimate the activation energy of petroleum coke combustion and found that the modified normal distribution function and the shrinking core model had the best fitting effect.

Received: August 1, 2022
Accepted: October 26, 2022
Published: November 3, 2022

In recent years, artificial neural networks have seen rapid development in the fields of energy and engineering technology due to their excellent generalization ability and computing speed, which can effectively solve problems that are difficult to handle by traditional experiments and simulations.[6,12,19−25] The application of artificial neural networks in petroleum coke pyrolysis has also been reported. For example, Govindan et al.[21] used a shrinking particle model and a weight fraction model to estimate the combustion kinetic parameters of calcined petroleum coke. This study focused on the isothermal pyrolysis of calcined petroleum coke at 650 °C and constructed an artificial neural network based on isothermal thermogravimetric analysis (TGA) data to predict the thermogravimetric (TG) curves of combustion and oxygen combustion of calcined petroleum coke. The experimental data were in good agreement with the predicted data. This set a precedent in the field of machine learning research on petroleum coke pyrolysis kinetics. Kang et al.[26] used three optimization algorithms of a feedforward backpropagation neural network to predict the cogasification reaction of petroleum coke with coal or biomass in a fluidized bed, indicating that particle swarm optimization algorithms have better predictive performance. Prabhakaran et al.[12] obtained the pyrolysis kinetic parameters of petroleum coke in an oxygen atmosphere by a model-free method and verified and optimized the thermal degradation behavior by multidisciplinary tools such as artificial neural networks. In this study, the temperature and heating rate were used as the input layer, and mass % was used as the output layer. However, the pyrolysis process of petroleum coke is affected not only by temperature and heating rate but also by the type of petroleum coke (volatile content, element composition, etc.), which should be further considered.

In the present study, the thermogravimetric properties of six kinds of petroleum coke at different heating rates were analyzed by nonisothermal TGA, and their kinetic parameters were obtained based on an independent parallel reaction (IPR) model. Taking temperature, heating rate, and type of petroleum coke (represented by the contents of C, H, N, and S) as the input layer and mass % as the output layer, a backpropagation neural network (BPNN) was applied to build the petroleum coke pyrolysis prediction model, and the prediction performance of the model was verified by experimental data. Furthermore, the prediction performance of BPNN for six kinds of petroleum coke and the reliability of these BPNN-predicted thermal data in further steps, such as the calculation of activation energy, were discussed. The purpose of this research is to explore the possibility of replacing the thermogravimetric experimental data with the predicted data. Thus, the research time and cost in determining the optimal pyrolysis and calcination conditions of petroleum coke, as well as reactor design and optimization in the later stage, can be reduced.

2. MATERIALS AND METHODOLOGY

2.1. Raw Materials. To make the research more widely representative, the samples used in this experiment were selected from six sources of petroleum coke: Fushun (FS), Fuyu (FY), Wuhan (WH), Zhenhai (ZH), Qilu (QL), and Shijiazhuang (SJZ) in China. The samples were ground through a 100-mesh sieve and dried at 150 °C for 48 h. The physical and chemical analyses of petroleum coke were carried out through proximate analysis and ultimate analysis. Proximate analysis was performed to obtain the content of moisture and volatile matter according to the E871-82 2006, E1755-01 2007, and E872-&82 2006 standards.[27,28] Ultimate analysis was implemented on an elemental analyzer (Elementar Analysensystem GmbH, Germany) to investigate the contents of C, H, N, and S in petroleum coke. The physicochemical properties of the six kinds of petroleum coke are listed in Table S1. It can be observed that the volatile content of FY petroleum coke was the highest at 13.63%, and that of FS petroleum coke was the lowest at only 10.48%. The micromorphology of FS petroleum coke was observed by field emission scanning electron microscopy (SEM, Tescan Mira 3 XH, Czech), as shown in Figure S1. It is indicated that the surface of petroleum coke was uneven and rough and had an obvious layered flow texture. Petroleum coke had a typical porous structure. These holes passed through each other and were elliptical with a size of approximately 400 μm.

2.2. Thermal Decomposition of Petroleum Coke. The mass loss under thermal decomposition of six kinds of petroleum coke (FS, FY, WH, ZH, QL, and SJZ) was studied by a thermogravimetric analyzer (STA-449F3 Jupiter of Netzsch). A nonisothermal TGA experiment was carried out at heating rates of 5, 10, 15, and 20 °C/min at temperatures in the range of 25−1300 °C. TG runs were implemented under programmed purging of high-purity nitrogen (99.999%) at a gas flow rate of 40 mL/min. The thermogravimetry experimental data were used to establish the database of the BPNN model.

Thermogravimetry−mass spectrometry (TG−MS) equipment was used to monitor the gas products generated in the pyrolysis process of FS petroleum coke in real time. The thermogravimetric analyzer SETSYS Evolution 16/18 was manufactured by SETARAM, France. The mass spectrometer OMNI star was manufactured by PFEIFFER, Germany. TG−MS pyrolysis experiments were performed at a heating rate of 10 °C/min in a temperature range of 25−1200 °C. The 10 ± 0.1 mg sample was placed in the analyzer under high-purity helium gas (99.999%). The flow rate of the purge gas was 50 mL/min, and the flow rate of the protective gas was 25 mL/min. The operating voltage was 70 eV, and the mass spectrometry scanning range was 0−200 amu.

2.3. Kinetics Study. *2.3.1. Theory of Kinetic Triplets.* Pyrolysis of petroleum coke is a complex chemical process with multiple reactions frequently occurring throughout the conversion process. The pyrolysis process of petroleum coke in an inert atmosphere can be simply summarized as follows

$$\text{petroleum coke(s)} \rightarrow \text{residual carbon(s)} + \text{volatile(g)} \quad (1)$$

The solid-state reaction rate equation for the pyrolysis of petroleum coke can be expressed as[29]

$$\frac{d\alpha}{dt} = k(T)f(\alpha) \quad (2)$$

$$\alpha = (m_0 - m_t)/(m_0 - m_\infty) \quad (3)$$

$$k(T) = k_0 \exp(-E/RT) \quad (4)$$

where α represents the conversion rate of petroleum coke; m_0, m_t, and m_∞ are the initial, t time and final mass of petroleum coke, respectively; $f(\alpha)$ is the reaction mechanism function; $k(T)$ is the rate constant; k_0 is the preexponential

https://doi.org/10.1021/acsomega.2c04866
ACS Omega 2022, 7, 41201−41211

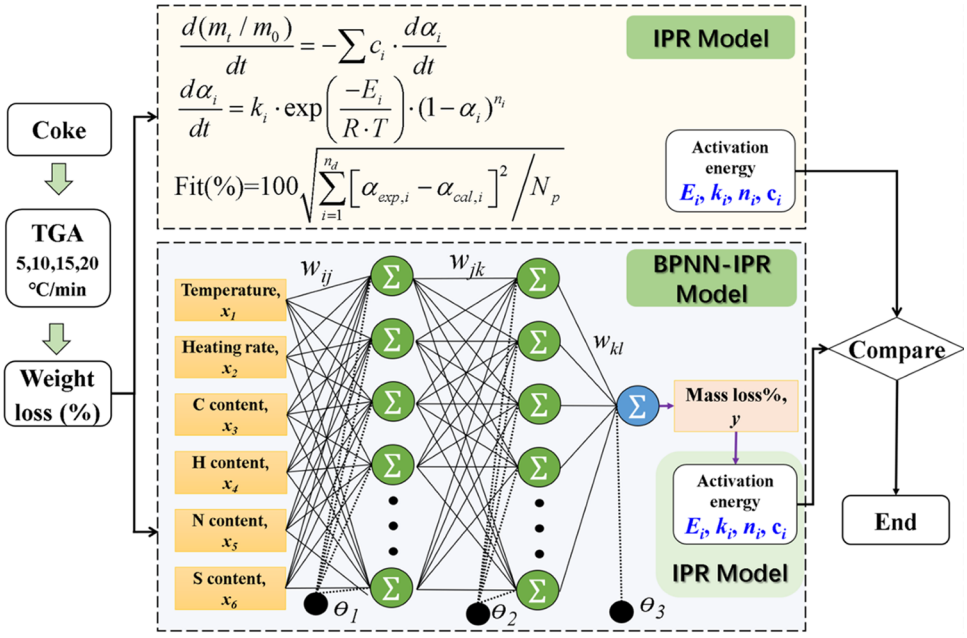

Figure 1. Overview of the methodology followed in this study.

factor; E is the apparent activation energy; R is the universal gas constant; and T is the temperature.

Under nonisothermal conditions, $\beta = dT/dt$. Then, eq 2 can be described as

$$\frac{d\alpha}{dT} = \frac{k_0}{\beta}\exp\left(-\frac{E}{RT}\right)f(\alpha) \tag{5}$$

Considering the pyrolysis reaction of petroleum coke as an isothermal homogeneous reaction, the differential form of $f(\alpha)$ can be expressed as $f(\alpha) = (1 - \alpha)^n$. Then, eq 5 can be rewritten as

$$\frac{d\alpha}{dT} = kf(\alpha) = \frac{k_0}{\beta}\exp\left(-\frac{E}{RT}\right)(1 - \alpha)^n \tag{6}$$

where n is the reaction order and β is the heating rate.

The integral form of $f(\alpha)$ of the nonisothermal thermal degradation of petroleum coke $g(\alpha)$ is as follows[30]

$$g(\alpha) = \int_0^\alpha \frac{d\alpha}{f(\alpha)} \approx \frac{k_0}{\beta}\int_0^T \exp\left(-\frac{E}{RT}\right)dT = \frac{k_0 E}{\beta R}p(y) \tag{7}$$

2.3.2. IPR Model. Petroleum coke has a porous structure, and its pyrolysis process is very complicated, including primary cracking (cracking and polycondensation of aromatic rings, breaking of branches and side chains of petroleum coke, etc.) and secondary reactions (tar cracking reaction and cross-linking to carbonization reaction).[31−33] These reactions are mostly parallel and sequential reactions, which can be modeled by the IPR model. The IPR model has been widely used in pyrolysis fields such as biomass and industrial waste, and relevant studies reported that model predictions agreed well with the experimental data.[34−36] The IPR model, also known as the n-pseudocomponent model, means that the pyrolysis process of petroleum coke can be described by several independent parallel first or nth reactions, each of which corresponds to the pyrolysis of different components in petroleum coke. This can be described as follows[37]

$$\frac{d(m_t/m_0)}{dt} = -\sum c_i \cdot \frac{d\alpha_i}{dt} \quad i = 1, 2, 3, \ldots N \tag{8}$$

$$\frac{d\alpha_i}{dt} = k_i \cdot \exp\left(-\frac{E_i}{R \cdot T}\right)\cdot(1 - \alpha_i)^{n_i} \tag{9}$$

where subscript i represents the ith pseudocomponent, and c_i is the mass fraction of pseudocomponent i.

The performance of the IPR model was evaluated by the fitting quality parameter Fit (%)[37]

$$\text{Fit}(\%) = 100\sqrt{\sum_{i=1}^{n_d}[\alpha_{\text{exp},i} - \alpha_{\text{cal},i}]^2/N_p} \tag{10}$$

where $\alpha_{\text{exp},i}$ and $\alpha_{\text{cal},i}$ represent the experimental data and calculated data, respectively, and N_p denotes the number of unknown parameters.

2.4. BPNN Methodology. BPNN is a typical multilayer feedforward artificial neural network. Structurally, the BPNN model contains input, hidden, and output layers. Each layer has neurons, and adjacent nodes are connected by weights, but the neurons in each layer are independent of each other. Its function process includes four parts: forward transmission of information, backward transmission of errors, circular memory training, and learning result discrimination. It was theoretically proven that a BPNN with a single hidden layer or a double hidden layer can approximate any nonlinear function with arbitrary precision and can well meet the needs of calculation in practical applications.[38−40] The main mathematical operation process of the BPNN model includes four steps, which are described in detail in eqs S1−S8 in the Supporting Information.[41]

In this work, first of all, a BPNN-based petroleum coke pyrolysis model with two hidden layers was established. In this model, the six variables of heating rate, temperature, and C, H, N, and S contents were used as the input layer, and the real-time mass % of petroleum coke was used as the output layer. The C, H, N, and S contents reflect the species characteristics of petroleum coke. In addition, BPNN-predicted mass loss

https://doi.org/10.1021/acsomega.2c04866
ACS Omega 2022, 7, 41201−41211

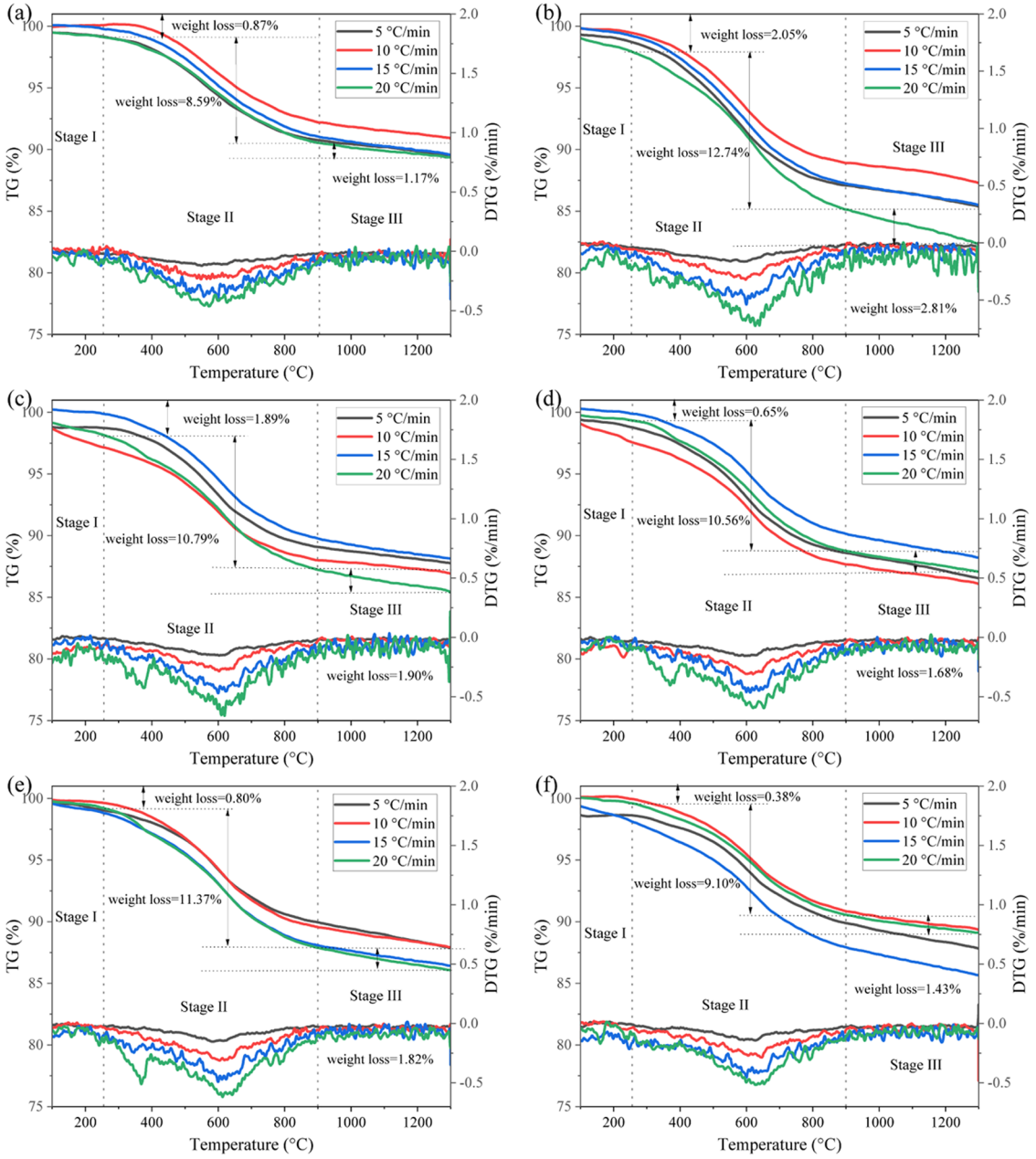

Figure 2. TG and DTG curves for six kinds of petroleum coke at heating rates of 5, 10, 15, and 20 °C/min: (a) FS, (b) FY, (c) WH, (d) ZH, (e) QL, and (f) SJZ.

data were applied to calculate pyrolytic activation energy based on the IPR model. The results were compared with the ones calculated using nonisothermal experimental data so as to evaluate the applicability and reliability of the BPNN model developed for a wide variety of petroleum coke. The overview of the methodology followed in this study is summarized in Figure 1.

3. RESULTS AND DISCUSSION

3.1. Pyrolysis Behavior of Petroleum Coke. The TG and differential thermogravimetric analysis (DTG) curves related to the pyrolysis of six kinds of petroleum coke (FS, FY, WH, ZH, QL, and SJZ) at heating rates of 5, 10, 15, and 20 °C/min under a nitrogen atmosphere are shown in Figure 2. The pyrolysis process of petroleum coke was divided into three stages. In stage I, physical and chemical changes such as drying, liquefaction, diffusion, and flow may occur, ranging from room temperature to 250 °C, and the mass loss was insignificant, which is only 0.87% for FS at a heating rate of 20 °C/min, as shown in Figure 2a. The maximum weight loss (8.59% in Figure 2a) can be observed in stage II, with a temperature range of 250−900 °C. The significant mass loss was attributed to the devolatilization of petroleum coke, accompanied by the release of a large amount of small-molecule volatiles, water, light oil, CO, and CO_2, which can be witnessed by a broad pyrolysis peak in the DTG curves. In stage III (900−1300 °C), the mass loss rate decreased significantly, and the weight loss was reduced to 1.17%, as shown in Figure 2a. This involved rapid polymerization and carbonization, and molecules rearranged petroleum coke, resulting in a disordered stacking structure that was more orderly and stable.

https://doi.org/10.1021/acsomega.2c04866
ACS Omega 2022, 7, 41201−41211

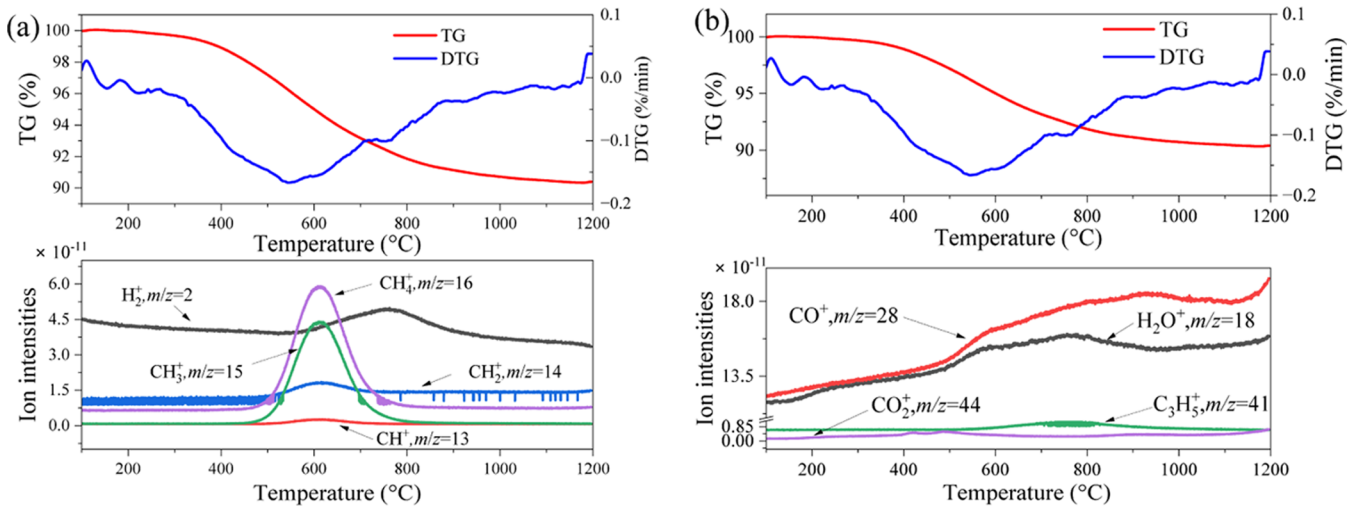

Figure 3. TG/DTG curves and MS fragmented ion intensities of pyrolysis products from thermal decomposition of FS petroleum coke: (a) H_2, m/z = 2; CH_x, m/z = 13, 14, 15, and 16; (b) H_2O, m/z = 18; CO, m/z = 28; C_3H_5, m/z = 41; CO_2, m/z = 44.

Table 1. Kinetic Parameters of Different Sources of Petroleum Coke Calculated Using the 3-IPR Model Based on Experimental Data

pseudocomponents	parameters	FS	FY	WH	ZH	QL	SJZ
1	$\ln(k_1)$ (s^{-1})	7.00	7.00	7.00	7.00	7.00	7.00
	E_1(kJ/mol)	92.36	86.40	87.96	91.97	91.88	92.74
	n_1	1.66	1.53	1.40	1.51	1.45	1.44
	c_1	0.41	0.34	0.37	0.42	0.42	0.42
2	$\ln(k_2)$ (s^{-1})	7.00	7.00	7.00	7.00	7.00	7.00
	E_2(kJ/mol)	73.52	66.30	66.20	67.66	67.89	67.81
	n_2	1.66	1.81	1.65	1.92	1.72	1.76
	c_2	0.23	0.19	0.17	0.21	0.21	0.19
3	$\ln(k_3)$ (s^{-1})	6.53	7.00	7.00	7.00	7.00	7.00
	E_3(kJ/mol)	111.15	105.82	107.82	115.28	115.77	118.20
	n_3	3.26	3.72	3.31	3.55	3.47	3.26
	c_3	0.36	0.47	0.45	0.37	0.37	0.38
fitting quality, fit (%)	R^2	>0.997	>0.999	>0.996	>0.997	>0.993	>0.993
	fit (%)	<0.030	<0.029	<0.040	<0.039	<0.046	<0.043

Moreover, the DTG curves of the six kinds of petroleum coke almost all had only one broad pyrolysis peak. Taking the pyrolysis of FS petroleum coke at 20 °C/min as an example, the pyrolysis started at approximately 250 °C, and the weight loss rate reached the maximum value of −0.4634 %/min at 572 °C. Until approximately 1300 °C, the pyrolysis basically ended, and the residual mass of petroleum coke was 89.36%. Among the six kinds of petroleum coke, FY petroleum coke had the largest value of weight loss and the maximum reaction rate. Combined with Table S1, it can be seen that this is due to the more intense pyrolysis reaction of FY petroleum coke with the highest volatile content. The residual proportion of FY petroleum coke was 82.34% when it underwent a non-isothermal procedure with a heating rate of 20 °C/min from room temperature to 1300 °C. In addition, it was found that a thermal hysteresis appeared in the DTG curve as the heating rate increased. The peak value of the DTG curves increased and shifted to the high-temperature region, due to the different conversion rates of petroleum coke at different heating rates.[37]

3.2. TG−MS Analysis of Petroleum Coke. Figure 3 illustrates the TG/DTG curves and the process and characteristics of the major small-molecule gas products released during the pyrolysis process of FS petroleum coke in the range of 100−1200 °C at a heating rate of 10 °C/min. As can be seen from Figure 3a, methane CH_x was one of the main aliphatic products of petroleum coke pyrolysis, which was dominated by m/z = 13, 14, 15, and 16 fragments in the mass spectrum. The CH_x fragments mainly appeared in stage II, which started to be generated at approximately 450 °C and reached their maximum precipitation peak at approximately 600 °C, which basically corresponds to the maximum pyrolysis peak (550 °C) in the TG/DTG curve. Of course, there was a small deviation due to the lag phenomenon in the gas precipitation process. They stopped generation at approximately 850 °C. Relevant research reported that CH_x was mainly produced by the cracking of aliphatic components in petroleum coke. The production process generally included the cleavage and decomposition of long-chain aryl−alkyl ether bonds, secondary cleavage, and other reactions.[42] In addition, an intensity peak of H_2 was also observed in the temperature range of 550−900 °C in stage II, which was mainly generated by the polycondensation of aromatic structures in petroleum coke.[43]

Figure 3b shows that C_3H_5 is the most important aliphatic hydrocarbon product, with a strong generation peak at approximately 800 °C, which corresponds exactly to the production peak of H_2. According to TG/DTG analysis, there

https://doi.org/10.1021/acsomega.2c04866
ACS Omega 2022, 7, 41201−41211

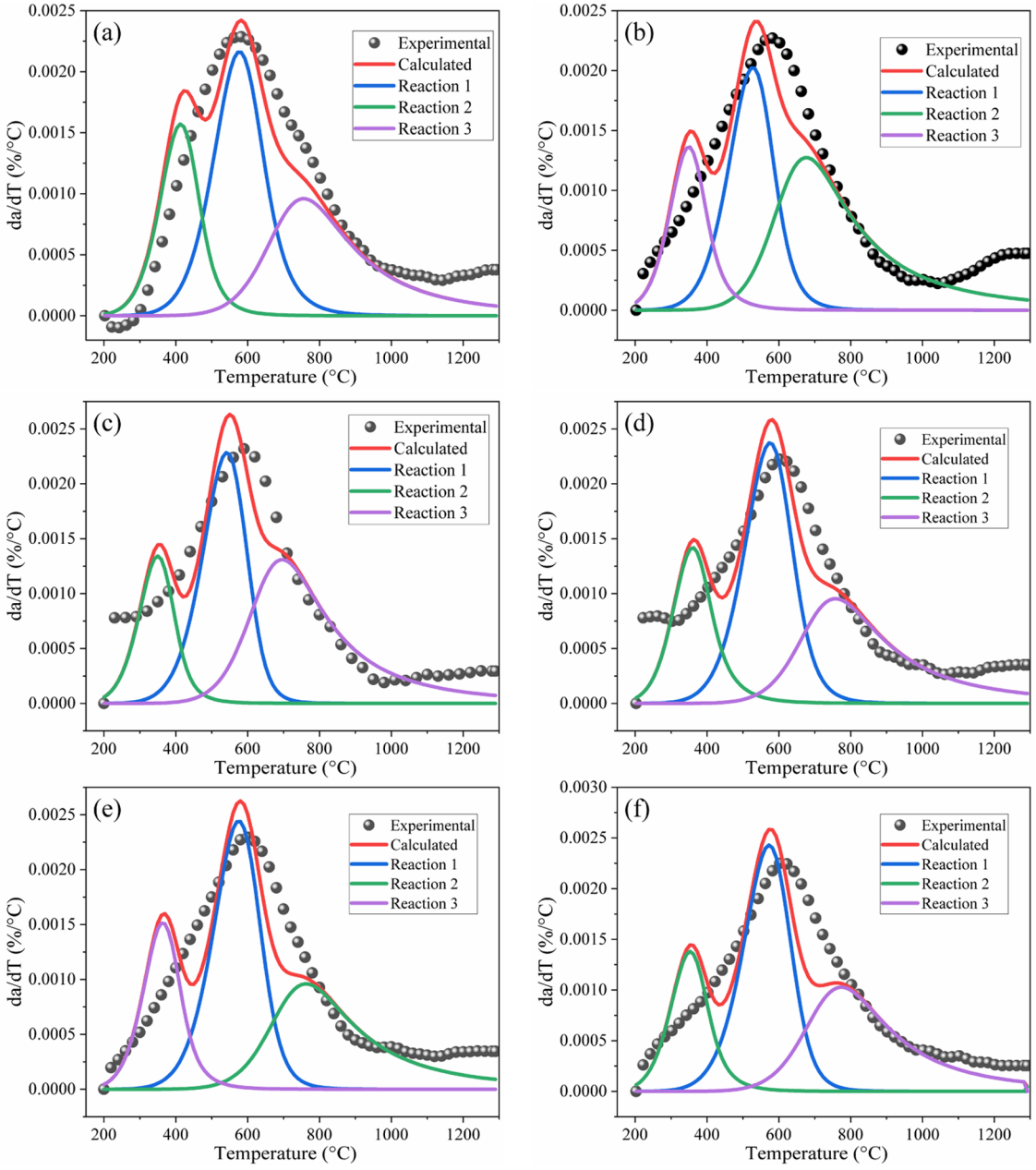

Figure 4. Experimental and calculated results by the 3-IPR model at a heating rate of 10 °C/min for (a) FS, (b) FY, (c) WH, (d) ZH, (e) QL, and (f) SJZ.

was just a small weight loss peak near 800 °C. C_3H_5 may arise from the breakdown of macromolecular functional groups in the structure of petroleum coke into smaller molecules. H_2O existed in the three stages. The water loss in stage I was related to the drying and precipitation of adsorbed water, and the water loss in the next two stages was related to the cracking of oxygen-containing functional groups (C−O and C−OH) in petroleum coke molecules. The higher peak range of H_2O generation (600−800 °C) corresponded to the strongest peaks of CH_x and C_3H_5, indicating that a large amount of H_2O is generated along with the production of CH_x and C_3H_5 during the pyrolysis of petroleum coke. Meanwhile, it was found that CO_2 mainly appeared at more than 200 °C and continued to exist until stage III. CO_2 in stage I was mainly the result of the precipitation of adsorbed CO_2. The strong and broad peak of CO_2 appeared in the temperature range of 400−600 °C in stage II, which was mainly due to the cleavage of aromatic weak bonds and oxygen-containing carboxyl functional groups.[42] The whole pyrolysis process of petroleum coke was accompanied by the release of a large amount of CO. According to relevant reports, CO may be generated from the decomposition of aliphatic ethers in the macromolecular structure of petroleum coke before 700 °C. However, when the temperature was higher than 700 °C, the generation of CO was mainly subject to Boudouard's equilibrium reaction.[44]

3.3. IPR Kinetics Calculation. An IPR model of three pseudocomponents (3-IPR) was used to successfully obtain the kinetic parameters (activation energy and preexponential factor), the content of each pseudocomponent, and the reaction order for six kinds of petroleum coke FS, FY, WH, ZH, QL, and SJZ, as shown in Table 1. Figure 4 presents the comparison of the experimental and calculated $d\alpha/dT$ results

https://doi.org/10.1021/acsomega.2c04866
ACS Omega 2022, 7, 41201−41211

of the six kinds of petroleum coke at a heating rate of 10 °C/min. The $d\alpha/dT$ curves calculated by the 3-IPR model were basically consistent with the experimental results. Of course, there was still a certain deviation, which is acceptable with a small fitting quality parameter Fit (%) of less than 0.046. The kinetic parameters of different petroleum coke species showed no significant difference. For pseudocomponent 1, the activation energies of FS, FY, WH, ZH, QL, and SJZ were 92.36, 86.40, 87.96, 91.97, 91.88, and 92.74 kJ/mol, respectively. For pseudocomponents 2 and 3, the activation energies of the six petroleum coke samples ranged from 66.20 to 73.52 and 105.82 to 118.20 kJ/mol, respectively. The reaction order of each pseudocomponent was also different. For pseudocomponents 1 and 2, the reaction order n was between 1.40 and 1.92. For pseudocomponent 3, the reaction order n was between 3.26 and 3.72.

3.4. Pyrolysis Prediction by the BPNN Model. In this work, the Tanh−Tanh combination was used as the activation function to establish a dual-hidden-layer BPNN model. The influence of the number of neurons in the hidden layer and the number of iterations on the performance of the model was examined by two parameters: mean squared error (MSE) and R^2. The variations in MSE and R^2 with the number of neurons in the hidden layer are shown in Figure 5. The MSE values of

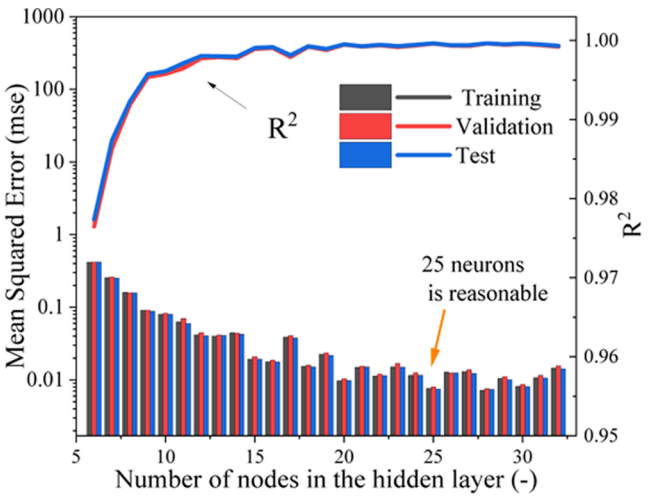

Figure 5. Variation in MSE and R^2 with the number of neurons in the hidden layer.

the training and validation sets were relatively small, and R^2 was close to 1 (R^2 = 0.9996) when the number of neurons in the hidden layer was 25. This result indicated that the degree of overfitting was relatively small when using this network structure. Therefore, the BP neural network model with double hidden layers established in this work had a topology of 6-25-25-1, which meant that the input layer had six nonlinear activation neurons, the two hidden layers each had 25 nonlinear activation neurons, and the output layer had one linear neuron.

Figure 6 shows the brief structure of the established BPNN model and the variation in MSE with the number of iterations during the training process. With an increase in the number of iterations, the MSE of the training, validation, and test decreased sharply at first, stabilized in the interval of 350−500 times, and then decreased rapidly. At 3000 iterations, the best validation performance of MSE = 0.01 for training was

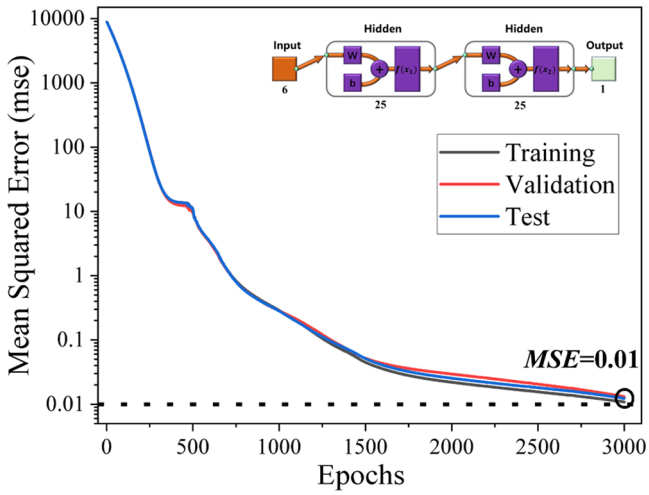

Figure 6. Variation in the MSE of training, validation, and test sets with the number of iterations.

achieved. The regression plots of the training data, validation data, test data, and complete data sets of the (6-25-25-1) BPNN model are presented in Figure 7. The regression coefficients for the training, validation, test, and entire data sets were all greater than 0.9989, indicating that the model predictions were very close to the experimental results. Therefore, the weight and bias vectors trained by the BPNN model can well describe the correlation between the petroleum coke species, heating rate, temperature, and mass% for the training samples.

In addition, the reliability of the BPNN-predicted thermal data in further steps was discussed. The kinetic parameters calculated by the 3-IPR model based on the BPNN-predicted thermal data are given in Table 2. Comparing Tables 1 and 2, the obtained activation energies were still close to the experimental ones, and the relative error was less than 8%. Therefore, it can be considered that using the thermal data predicted by BPNN combined with the IPR (BPNN-IPR) model can be effective and helpful for the prediction of the activation energy of the overall pyrolysis process of petroleum coke. Figure 8 shows the comparison of experimental data and the thermal data predicted by different models. As given in Figure 8, the IPR, BPNN, and BPNN-IPR predicted that α curves were very close to the experimental data. Of course, there were slight deviations between experimental and predicted data for six kinds of petroleum coke, due to the differences in their own theories and assumptions between different models. However, the deviations were less than 3%, which was acceptable. At this point, it was concluded that the BPNN can be an alternative and promising tool that allows for predicting thermal data and the further calculation of kinetic parameters.

4. CONCLUSIONS

TG and DTG analyses of FS, FY, WH, ZH, QL, and SJZ petroleum coke were implemented by the nonisothermal thermogravimetric method at heating rates of 5, 10, 15, and 20 °C/min. The results showed that the thermogravimetric trends of the six kinds of petroleum coke were basically similar, and the DTGs of different petroleum coke had a single broad pyrolysis peak. The pyrolysis process was divided into three stages, of which the temperature range of 250−900 °C was the

https://doi.org/10.1021/acsomega.2c04866
ACS Omega 2022, 7, 41201−41211

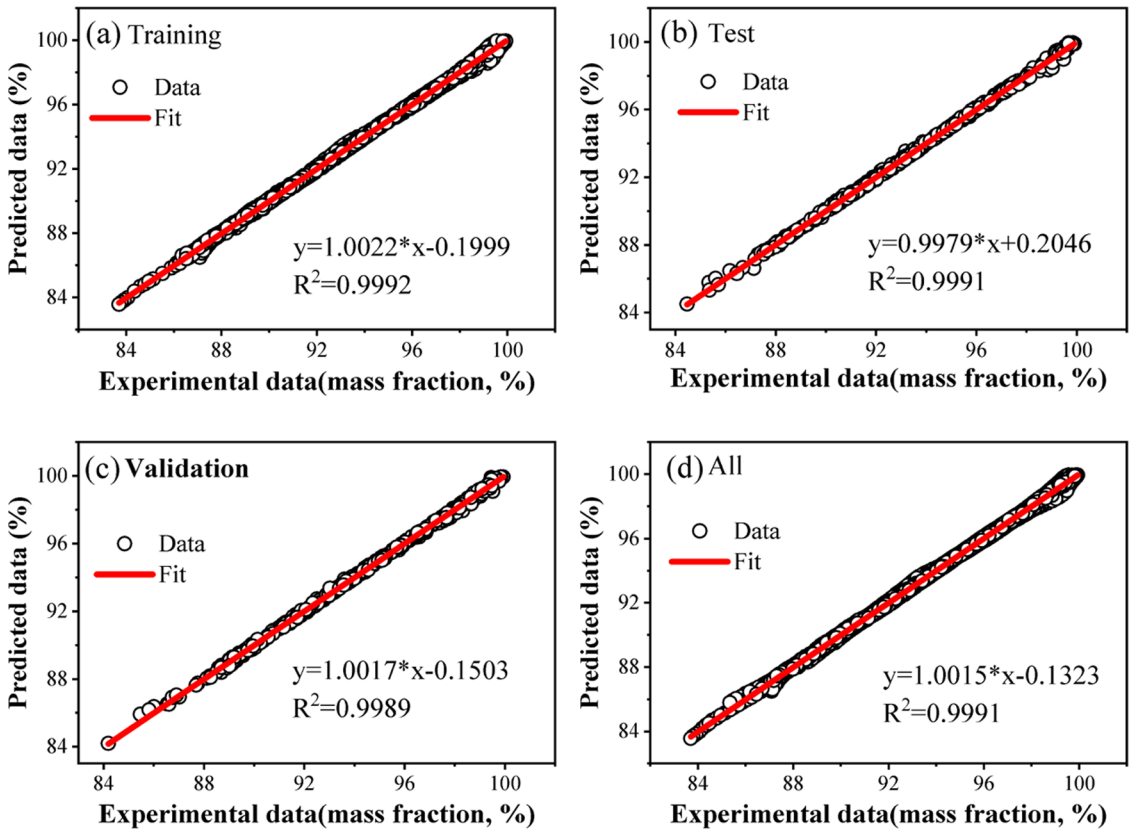

Figure 7. Regression plots of (a) training data, (b) validation data, (c) test data, and (d) complete data sets of the (6-25-25-1) BPNN model.

Table 2. Kinetic Parameters of Six Kinds of Petroleum Coke Calculated Using the 3-IPR Model Based on BPNN-Predicted Thermal Data

pseudocomponents	parameters	FS	FY	WH	ZH	QL	SJZ
1	$\ln(k_1)$ (s^{-1})	7.00	7.00	7.00	7.00	7.00	7.00
	E_1(kJ/mol)	90.55	85.27	85.38	92.55	87.77	88.63
	n_1	1.20	1.37	0.65	1.36	1.26	0.70
	c_1	0.35	0.32	0.21	0.37	0.31	0.23
2	$\ln(k_2)$ (s^{-1})	7.00	7.00	7.00	7.00	7.00	7.00
	E_2(kJ/mol)	73.44	63.79	65.16	68.03	65.39	68.72
	n_2	1.26	1.68	1.18	1.76	1.27	1.17
	c_2	0.20	0.15	0.15	0,22	0.16	0.15
3	$\ln(k_3)$ (s^{-1})	7.00	7.00	7.00	7.00	7.00	7.00
	E_3(kJ/mol)	110.71	103.33	101.57	112.85	106.76	106.69
	n_3	3.12	3.58	3.19	3.64	3.63	3.55
	c_3	0.45	0.52	0.64	0.41	0.53	0.62

main weight loss interval, corresponding to the devolatilization of petroleum coke. The process and characteristics of gas products in the pyrolysis process of petroleum coke were investigated by a TG−MS device. MS fragmented ion intensity analysis indicated that the main pyrolysis products were methane CH_x (m/z = 13, 14, 15, and 16), aliphatic hydrocarbon C_3H_5, H_2, CO, CO_2, and H_2O.

The 3-IRP model was used to simulate the pyrolysis process of six kinds of petroleum coke. The results showed that the kinetic parameters of the pseudocomponents of the six kinds of petroleum coke showed no significant difference, and the activation energies of pseudocomponents 1, 2, and 3 ranged from 86.40 to 92.74, 66.20 to 73.52, and 105.82 to 118.20 kJ/mol, respectively. For pseudocomponents 1 and 2, the reaction order n was between 1.40 and 1.92; for pseudocomponent 3, the reaction order n was between 3.26 and 3.72.

An efficient BPNN tool with a network topology of 6-25-25-1 was developed to predict the TGA kinetic data of petroleum coke. In this model, the six variables of heating rate, temperature, and C, H, N, and S contents were used as the input layer and the mass % of petroleum coke in real time was used as the output layer. The Tanh−Tanh combination was used as the activation function. The results showed that the data predicted by the model were in good agreement with the experimental data, with very high regression coefficient values (R^2 > 0.9989). Moreover, based on the IPR model, the activation energies calculated from the thermal data predicted by BPNN were close to the ones obtained from the experimental data. The thermal data predicted by the IPR,

https://doi.org/10.1021/acsomega.2c04866
ACS Omega 2022, 7, 41201−41211

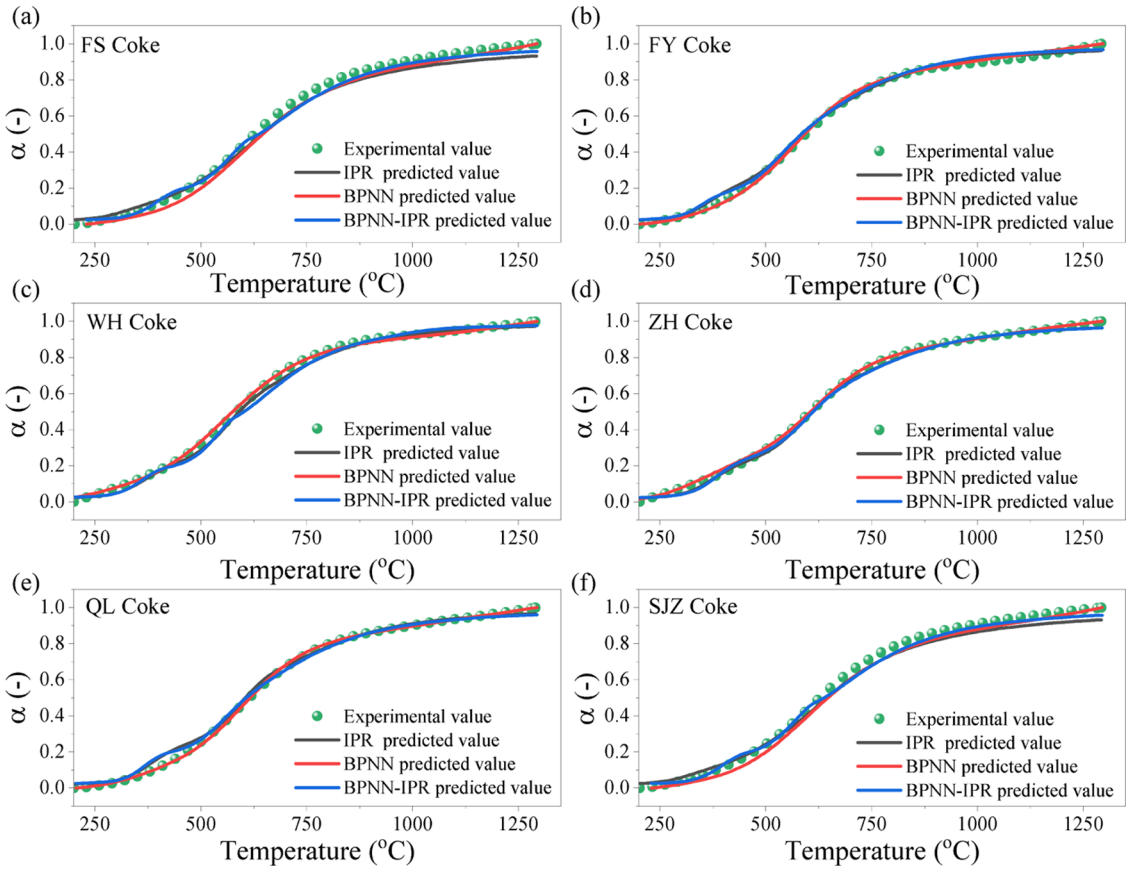

Figure 8. Comparison between conversion rate (α) curves predicted by different models (IPR, BPNN, and BPNN-IPR) and experimental data for 10 °C/min: (a) FS, (b) FY, (c) WH, (d) ZH, (e) QL, and (f) SJZ.

BPNN, and BPNN-IPR models were in good agreement with the experimental data. Therefore, it was concluded that the BPNN-predicted thermal data were alternative and applicable to the subsequent calculation of kinetic parameters.

■ ASSOCIATED CONTENT

Supporting Information

The Supporting Information is available free of charge at https://pubs.acs.org/doi/10.1021/acsomega.2c04866.

SEM images for FS petroleum coke sample; physicochemical properties of six kinds of petroleum coke, and description of BPNN methodology (Figure S1, Table S1, and Equations S1−S8) (PDF)

■ AUTHOR INFORMATION

Corresponding Author

Jing Li − *Faculty of Materials Metallurgy and Chemistry, Jiangxi University of Science and Technology, Ganzhou, Jiangxi 341000, China; School of Metallurgical Engineering, Jiangxi University of Science and Technology, Ganzhou, Jiangxi 341000, China;* orcid.org/0000-0002-6099-8349; Email: 9120200008@jxust.edu.cn

Authors

Jindi Huang − *Faculty of Materials Metallurgy and Chemistry, Jiangxi University of Science and Technology, Ganzhou, Jiangxi 341000, China; School of Metallurgical Engineering, Jiangxi University of Science and Technology, Ganzhou, Jiangxi 341000, China;* orcid.org/0000-0002-3679-0986

Zhihang Chen − *Faculty of Materials Metallurgy and Chemistry, Jiangxi University of Science and Technology, Ganzhou, Jiangxi 341000, China*

Dou Zhang − *Faculty of Materials Metallurgy and Chemistry, Jiangxi University of Science and Technology, Ganzhou, Jiangxi 341000, China*

Complete contact information is available at: https://pubs.acs.org/10.1021/acsomega.2c04866

Notes

The authors declare no competing financial interest.

■ ACKNOWLEDGMENTS

This work was financially supported by the National Natural Science Foundation of China (52004112), the Science and Technology Program of Education Department of Jiangxi Province in China (GJJ200848), the Program of Qingjiang Excellent Young Talents of Jiangxi University of Science and Technology (JXUSTQJYX2020016), and the Scientific Research Foundation of Jiangxi University of Science and Technology (205200100517).

■ REFERENCES

(1) Yang, H.; Song, H.; Zhao, C.; Hu, J.; Li, S.; Chen, H. Catalytic Gasification Reactivity and Mechanism of Petroleum Coke at High Temperature. *Fuel* **2021**, *293*, No. 120469.

(2) Leion, H.; Mattisson, T.; Lyngfelt, A. The Use of Petroleum Coke as Fuel in Chemical-Looping Combustion. *Fuel* **2007**, *86*, 1947−1958.

(3) Wang, J.; Anthony, E. J.; Abanades, J. C. Clean and Efficient Use of Petroleum Coke for Combustion and Power Generation. *Fuel* **2004**, *83*, 1341−1348.
(4) Okeke, I. J.; Adams, T. A., II Combining Petroleum Coke and Natural Gas for Efficient Liquid Fuels Production. *Energy* **2018**, *163*, 426−442.
(5) Murthy, B. N.; Sawarkar, A. N.; Deshmukh, N. A.; Mathew, T.; Joshi, J. B. Petroleum Coke Gasification: A Review. *Can. J. Chem. Eng.* **2014**, *92*, 441−468.
(6) Merdun, H.; Sezgin, I. V. Modelling of Pyrolysis Product Yields by Artificial Neural Networks. *Int. J. Energy Res.* **2018**, *8*, 1178−1188.
(7) He, Q.; Yu, J.; Song, X.; Ding, L.; Wei, J.; Yu, G. Utilization of Biomass Ash for Upgrading Petroleum Coke Gasification: Effect of Soluble and Insoluble Components. *Energy* **2020**, *192*, No. 116642.
(8) Ba, Z.; Zhao, J.; Li, C.; Huang, J.; Fang, Y.; Zhang, L.; Kong, L.; Wang, Q. Developing Efficient Gasification Technology for High-Sulfur Petroleum Coke to Hydrogen-Rich Syngas Production. *Fuel* **2020**, *267*, No. 117170.
(9) Gajera, Z. R.; Verma, K.; Tekade, S. P.; Sawarkar, A. N. Kinetics of Co-Gasification of Rice Husk Biomass and High Sulphur Petroleum Coke with Oxygen as Gasifying Medium via TGA. *Bioresour. Technol. Rep.* **2020**, *11*, No. 100479.
(10) Manasrah, A. D.; Nassar, N. N.; Ortega, L. C. Conversion of Petroleum Coke into Valuable Products Using Oxy-Cracking Technique. *Fuel* **2018**, *215*, 865−878.
(11) Shan, Y.; Guan, D.; Meng, J.; Liu, Z.; Schroeder, H.; Liu, J.; Mi, Z. Rapid Growth of Petroleum Coke Consumption and Its Related Emissions in China. *Appl. Energy* **2018**, *226*, 494−502.
(12) S P, S. P.; G, S.; Joshi, V. V. Thermogravimetric Analysis of Hazardous Waste: Pet-Coke, by Kinetic Models and Artificial Neural Network Modeling. *Fuel* **2021**, *287*, No. 11940.
(13) Tripathi, N.; Singh, R. S.; Hills, C. D. Microbial Removal of Sulphur from Petroleum Coke (Petcoke). *Fuel* **2019**, *235*, 1501−1505.
(14) Huang, J.; Li, J.; Li, M.; Yan, K. Orthogonal Design-Based Grey Relational Analysis for Influence of Factors on Calcination Temperature in Shaft Calciner. *J. Chem. Eng. Jpn.* **2019**, *52*, 811−821.
(15) Xiao, J.; Zhang, Y.; Zhong, Q.; Li, F.; Huang, J.; Wang, B. Reduction and Desulfurization of Petroleum Coke in Ammonia and Their Thermodynamics. *Energy Fuel* **2016**, *30*, 3385−3391.
(16) Xiao, J.; Li, F.; Zhong, Q.; Huang, J.; Wang, B.; Zhang, Y. Effect of High-Temperature Pyrolysis on the Structure and Properties of Coal and Petroleum Coke. *J. Anal. Appl. Pyrolysis* **2016**, *117*, 64−71.
(17) Shen, B.-X.; Liu, D.; Chen, H. A Study of the Mechanism of Petroleum Coke Pyrolysis. *Dev. Chem. Eng. Miner. Process.* **2008**, *8*, 351−358.
(18) Afrooz, I. E.; Ching, D. L. C. A Modified Model for Kinetic Analysis of Petroleum Coke. *Int. J. Chem. Eng.* **2019**, *2019*, 1−8.
(19) Xing, J.; Luo, K.; Pitsch, H.; Wang, H.; Bai, Y.; Zhao, C.; Fan, J. Predicting Kinetic Parameters for Coal Devolatilization by Means of Artificial Neural Networks. *Proc. Combust. Inst.* **2019**, *37*, 2943−2950.
(20) Dubdub, I.; Al-Yaari, M. Pyrolysis of Low Density Polyethylene: Kinetic Study Using TGA Data and ANN Prediction. *Polymers* **2020**, *12*, No. 891.
(21) Govindan, B.; Jakka, S. C. B.; Radhakrishnan, T. K.; Tiwari, A. K.; Sudhakar, T. M.; Shanmugavelu, P.; Kalburgi, A. K.; Sanyal, A.; Sarkar, S. Investigation on Kinetic Parameters of Combustion and Oxy-Combustion of Calcined Pet Coke Employing Thermogravimetric Analysis Coupled to Artificial Neural Network Modeling. *Energy Fuels* **2018**, *32*, 3995−4007.
(22) Wei, H.; Luo, K.; Xing, J.; Fan, J. Predicting Co-Pyrolysis of Coal and Biomass Using Machine Learning Approaches. *Fuel* **2022**, *310*, No. 122248.
(23) Al-Yaari, M.; Dubdub, I. Pyrolytic Behavior of Polyvinyl Chloride: Kinetics, Mechanisms, Thermodynamics, and Artificial Neural Network Application. *Polymers* **2021**, *13*, No. 4359.
(24) Muravyev, N. V.; Luciano, G.; Ornaghi, H. L.; Svoboda, R.; Vyazovkin, S. Artificial Neural Networks for Pyrolysis, Thermal Analysis, and Thermokinetic Studies: The Status Quo. *Molecules* **2021**, *26*, No. 3727.
(25) Hough, B. R.; Beck, D. A. C.; Schwartz, D. T.; Pfaendtner, J. Application of Machine Learning to Pyrolysis Reaction Networks: Reducing Model Solution Time to Enable Process Optimization. *Comput. Chem. Eng.* **2017**, *104*, 56−63.
(26) Kang, J.; Zhao, L.; Li, W.; Song, Y. Artificial Neural Network Model of Co-Gasification of Petroleum Coke with Coal or Biomass in Bubbling Fluidized Bed. *Renewable Energy* **2022**, *194*, 359−365.
(27) Naqvi, S. R.; Tariq, R.; Hameed, Z.; Ali, I.; Taqvi, S. A.; Naqvi, M.; Niazi, M. B. K.; Noor, T.; Farooq, W. Pyrolysis of High-Ash Sewage Sludge: Thermo-Kinetic Study Using TGA and Artificial Neural Networks. *Fuel* **2018**, *233*, 529−538.
(28) Yousef, S.; Eimontas, J.; Striūgas, N.; Abdelnaby, M. A. Modeling of Metalized Food Packaging Plastics Pyrolysis Kinetics Using an Independent Parallel Reactions Kinetic Model. *Polymers* **2020**, *12*, No. 1763.
(29) Sun, Y.; Bai, F.; Lü, X.; Jia, C.; Wang, Q.; Guo, M.; Li, Q.; Guo, W. Kinetic Study of Huadian Oil Shale Combustion Using a Multi-Stage Parallel Reaction Model. *Energy* **2015**, *82*, 705−713.
(30) Bai, F.; Guo, W.; Lü, X.; Liu, Y.; Guo, M.; Li, Q.; Sun, Y. Kinetic Study on the Pyrolysis Behavior of Huadian Oil Shale via Non-Isothermal Thermogravimetric Data. *Fuel* **2015**, *146*, 111−118.
(31) Zhong, Q.; Mao, Q.; Zhang, L.; Xiang, J.; Xiao, J.; Mathews, J. P. Structural Features of Qingdao Petroleum Coke from Hrtem Lattice Fringes: Distributions of Length, Orientation, Stacking, Curvature, and a Large-Scale Image-Guided 3D Atomistic Representation. *Carbon* **2018**, *129*, 790−802.
(32) Yu, X.; Yu, D.; Yu, G.; Liu, F.; Han, J.; Wu, J.; Xu, M. Temperature-Resolved Evolution and Speciation of Sulfur during Pyrolysis of a High-Sulfur Petroleum Coke. *Fuel* **2021**, *295*, No. 120609.
(33) Yu, X.; Yu, D.; Liu, F.; Wu, J.; Xu, M. High-Temperature Pyrolysis of Petroleum Coke and Its Correlation to In-Situ Char-CO_2 Gasification Reactivity. *Proc. Combust. Inst.* **2021**, *38*, 3995−4003.
(34) Santos, K. G.; Lobato, F. S.; Lira, T. S.; Murata, V. V.; Barrozo, M. A. S. Sensitivity Analysis Applied to Independent Parallel Reaction Model for Pyrolysis of Bagasse. *Chem. Eng. Res. Des.* **2012**, *90*, 1989−1996.
(35) Chen, F.; Zhang, F.; Yang, S.; Liu, H.; Wang, H.; Hu, J. Investigation of Non-Isothermal Pyrolysis Kinetics of Waste Industrial Hemp Stem by Three-Parallel-Reaction Model. *Bioresour. Technol.* **2022**, *347*, No. 126402.
(36) Sfakiotakis, S.; Vamvuka, D. Development of a Modified Independent Parallel Reactions Kinetic Model and Comparison with the Distributed Activation Energy Model for the Pyrolysis of a Wide Variety of Biomass Fuels. *Bioresour. Technol.* **2015**, *197*, 434−442.
(37) Li, J.; Huang, J. Thermal Debinding Kinetics of Gelcast Ceramic Parts via a Modified Independent Parallel Reaction Model in Comparison with the Multiple Normally Distributed Activation Energy Model. *ACS Omega* **2022**, *7*, 20219−20228.
(38) Li, Q.; Xu, Z. Y. Parameter Identification Method Research Based on the BP Neural Network and Space Search. *Appl. Mech. Mater.* **2014**, *513*−*517*, 1165−1169.
(39) Wu, Y.; Zeng, Z. A Rapid Detection Method of Earthquake Infrasonic Wave Based on Decision-Making Tree and the BP Neural Network. *Int. J. Inf. Comumun. Technol.* **2019**, *14*, 295−307.
(40) Li, J.; Yao, X.; Ge, J.; Yu, Y.; Yang, D.; Chen, S.; Xu, K.; Geng, L. Investigation on the Pyrolysis Process, Products Characteristics and BP Neural Network Modelling of Pine Sawdust, Cattle Dung, Kidney Bean Stalk and Bamboo. *Process Saf. Environ. Prot.* **2022**, *162*, 752−764.
(41) Ashraf, M.; Aslam, Z.; Ramzan, N.; Aslam, U.; Durrani, A. K.; Khan, R. U.; Ayaz, S. Pyrolysis of Cattle Dung: Model Fitting and Artificial Neural Network Validation Approach. *Biomass Convers. Biorefin.* **2021**, 1−12.
(42) Wang, M.; Li, Z.; Huang, W.; Yang, J.; Xue, H. Coal Pyrolysis Characteristics by TG-MS and Its Late Gas Generation Potential. *Fuel* **2015**, *156*, 243−253.

https://doi.org/10.1021/acsomega.2c04866
ACS Omega 2022, 7, 41201−41211

(43) Campbell, J. H. Pyrolysis of Subbituminous Coal in Relation to In-Situ Coal Gasification. *Fuel* **1978**, *57*, 224−271.
(44) Siskin, M.; Aczel, T. Pyrolysis Studies on the Structure of Ethers and Phenols in Coal. *Fuel* **1983**, *62*, 1321−1326.

https://doi.org/10.1021/acsomega.2c04866
ACS Omega 2022, 7, 41201−41211